Intermolecular potential energy surface and second virial coefficients for the nonrigid water-CO dimer

Richard J. Wheatley[1,a] and Allan H. Harvey[2,b]
[1]*School of Chemistry, The University of Nottingham, Nottingham NG7 2RD, United Kingdom*
[2]*Thermophysical Properties Division, National Institute of Standards and Technology, Boulder, Colorado 80305, USA*

(Received 3 August 2009; accepted 17 September 2009; published online 19 October 2009)

A seven-dimensional potential energy surface is calculated for the interaction of water and carbon monoxide using second-order Møller–Plesset theory, coupled-cluster theory, and extrapolated intermolecular perturbation theory. The effects of stretching the CO molecule and bending the water molecule are included. The minimum energy structure of the water-CO dimer changes from an H–C hydrogen bond to an H–O hydrogen bond when the CO bond length increases by less than 10 pm from its equilibrium value. Second virial coefficients for the water-CO interaction are calculated for a wide range of temperatures and compared with the limited experimental data. Allowing the CO bond length and water bond angle to vary has little effect on the second virial coefficients. © *2009 American Institute of Physics*. [doi:10.1063/1.3244594]

I. INTRODUCTION

The weak intermolecular bond formed between water and carbon monoxide is of considerable theoretical and experimental interest. Water and CO are common and important molecules, which are found together in the Earth's atmosphere, in the products of combustion reactions, and in the interstellar medium. Structurally and energetically, the intermolecular bond in the water-CO dimer resembles a weak hydrogen bond, but the dipole moment of CO is so small that either end of the CO molecule can be attracted to the hydrogen atoms of water, and the weakness of the bond means that a large fraction of the potential well, including regions far away from the equilibrium structures, must be considered in understanding the properties of the dimer.

Carbon monoxide is present in many important industrial processes. The water-CO binary is relevant for the important water-gas shift reaction and in the production of synthesis gas (consisting mostly of CO and H_2) from gasification of coal or biomass. In the Integrated Gasification Combined Cycle (IGCC) power cycle that facilitates precombustion separation of CO_2 for sequestration, a key step in some designs is quenching the hot synthesis gas with water. The vapor-liquid equilibrium of this step is important to the economics; a key factor in this equilibrium is the nonideal vapor-phase interaction between water and the synthesis gases, which can be modeled accurately if the interaction second virial coefficients between water and the gas components are known.[1]

The water-CO dimer has been observed using microwave and far-infrared spectroscopy,[2,3] and using infrared spectroscopy in the region of the CO stretch[4] and the water asymmetric stretch.[5] The results give information on the lowest-energy equilibrium structure of the dimer, which features a weak hydrogen bond between the C atom of CO and one H atom of water, with a separation of approximately 241 pm between the two atoms.[2] The potential energy surface away from the minimum is much less well characterized experimentally. Information on the barrier height for interconversion of the two hydrogen atoms has been estimated from a model Hamiltonian to be around 210–230 cm^{-1} from the tunneling splittings in the microwave spectrum.[2,3] The barrier height decreases when the CO stretch is excited, which also weakens the intermolecular bond.[4] However, the multidimensional nature of the tunneling complicates the analysis of the spectra, and the use of a simplified model Hamiltonian, as well as the assumptions made in earlier work that the tunneling splitting is independent of the rotational quantum number K_a, cannot be justified.[5] More theoretical work on developing a full multidimensional potential energy surface is essential for an understanding of the dimer spectrum.[5]

Computational work on the dimer has also been concerned primarily with the minimum energy structure(s). The calculations of Sadlej and co-workers[6,7] identified two planar minimum energy structures. The experimental structure was predicted to be the most strongly bound, and a hydrogen bond between the O atom of CO and an H atom of water was also predicted to be a local minimum. A third planar structure, in which the O atom of water approaches the middle of the C–O bond, was not found to be a minimum. The blueshift of the CO stretching frequency for the equilibrium dimer structure, compared with its value for the CO monomer, was predicted correctly.

A subsequent calculation of the equilibrium structure of the dimer using the Møller–Plesset MP2 method with a fairly small basis set[8] agreed with previous predictions of a near-linear O–C···H–O hydrogen bonded structure and gave an intermolecular bond energy of $D_e \approx 7.0$ kJ mol^{-1}. Most recently, density functional theory has been used[9] to compute harmonic and anharmonic frequencies of the dimer, but the

[a]Electronic mail: richard.wheatley@nottingham.ac.uk.
[b]Electronic mail: aharvey@boulder.nist.gov.

results are not in good agreement with the experimental data. Inclusion of electron correlation using the CR-CC(2,3) method gave an intermolecular bond energy of $D_e \approx 8.4$ kJ mol^{-1}, which is in reasonable agreement[9] with experiment.

The aim of this work is to improve on previous studies by providing complete coverage of all accessible regions of the water-CO potential energy surface, not just regions around the minima. It is hoped that this will allow a more complete assignment of existing spectroscopic data for the dimer. The effect of the one-particle basis set on the energy is also investigated, and the results are extrapolated to the infinite basis set limit. A higher level of electron correlation is used than in previous studies, including a number of coupled-cluster calculations and the calculation of a complete potential energy surface with extrapolated intermolecular perturbation theory. Finally, since the dipole moment of CO changes qualitatively with its bond length, calculations are also performed for nonequilibrium monomer geometries to investigate what effect monomer geometry has on the intermolecular potential energy surface. The water bond angle and CO bond length are both varied in the calculations, as these correspond to the lowest-frequency vibrational modes of the monomers, and may therefore be expected to be most affected by temperature. This nonrigid surface may also help to interpret the infrared spectrum of the dimer in the CO stretching region. The methodology and the main features of the potential energy surface are described in Secs. II and III. The potential energy surface is also used to calculate second virial coefficients for the water-CO binary mixture, and the results are presented and discussed in Secs. IV and V.

II. METHODOLOGY

Potential energy surfaces for the H_2O-CO dimer are initially calculated with the supermolecule second-order Møller–Plesset (MP2) method with the aug-cc-pVTZ and aug-cc-pVQZ basis sets[10] and full counterpoise correction. In total, 13 different pairs of intramolecular geometries are considered. Four water bond angles (80°, 100°, 120°, and 140°) are used in all possible combinations with three CO bond lengths (2.0, 2.175, and 2.35 a_0, where the Bohr radius is $a_0 \approx 52.917\ 72$ pm) to give 12 pairs. The monomer OH bond lengths in water are chosen for each water bond angle x by calculating MP2/aug-cc-pVQZ water monomer energies at a range of OH bond lengths from 1.5 to 2.5a_0 (both OH bonds being the same length), fitting the result to a polynomial in the bond length, and solving a one-dimensional Schrödinger equation for the symmetric stretching motion on the fitted surface with a reduced mass of $2m_H m_O/(2m_H \cos^2(x/2) + m_O)$, where m_H and m_O are the atomic masses. The OH bond lengths are taken to be the expectation value of the bond length in the resulting ground-state wave function. This is 1.8626 a_0 for $x=80°$, 1.8327 a_0 for $x=100°$, 1.8146 a_0 for $x=120°$, and 1.8004 a_0 for $x=140°$.

The 13th pair of intramolecular geometries uses vibrational ground-state geometries for the two monomers with an OH bond length in water of 1.8361 a_0, an HOH bond angle of 104.69°,[11] and a CO bond length of 2.132 a_0.[12]

For each of the two basis sets, the MP2 intermolecular potential is calculated at more than 10000 relative intermolecular geometries for each of the 13 intramolecular pairs. The intermolecular geometries include 13 different separations between the geometrical bond center of CO and the oxygen atom of water from a minimum of 4 a_0 to 8 a_0 in steps of 0.5 a_0, as well as 9, 10, 11, and 12 a_0. These are combined with 930 relative intermolecular orientations, which are chosen to be the same as the 465 water-O_2 relative orientations used in previous work,[13] with an extra factor of 2 reflecting the fact that O_2 can be replaced with CO pointing in two opposite directions. The MOLPRO program[14,15] is used for the MP2 calculations. A few high-energy points, corresponding to very close intermolecular contacts, are removed from the resulting data.

The MP2 supermolecule method does not usually give potential energy surfaces of sufficient quality to yield reliable thermodynamic data, and the use of the MP2 method is particularly questionable for dimers involving CO because of the large relative correlation correction to the CO dipole. Coupled-cluster calculations with single, double, and perturbative triple excitations [CCSD(T)] are therefore performed with the aug-cc-pVTZ basis set. However, CCSD(T) calculations with the aug-cc-pVQZ basis set proved to be infeasible, and the high computational cost of the aug-cc-pVTZ calculations restricts their use to a total of 120 points on the complete seven-dimensional surface. Based on previous work and on a study of the MP2 results, these points are chosen to comprise five intermolecular distances from 5 to 9 a_0 in steps of 1 a_0, water bond angles of 80° and 120°, CO bond lengths of 2.175 and 2.35 a_0, and seven planar intermolecular geometries: four different geometries near the CO–H and OC–H hydrogen-bonded minima, one geometry with the middle of the CO bond near the water oxygen atom, and two geometries of C_{2v} symmetry with the CO molecule on the water symmetry axis, at the end nearer the hydrogen atoms, one with the C end and one with the O end of the CO molecule pointing toward the water molecule. Of these 140 geometries, 20 are not used as they have close intermolecular contacts and large, repulsive intermolecular potentials.

An alternative way of improving the treatment of electron correlation in weak intermolecular complexes is by the use of intermolecular perturbation theory. The systematic intermolecular potential extrapolation routine (SIMPER) method[16] has been used to calculate potential energy surfaces in good agreement with experimental data, and to calculate second virial coefficients for mixtures of water with H_2,[17] N_2,[18] and O_2.[13] In the present work, a slightly modified version of the SIMPER method is used. The MP2 supermolecule energy is divided into electrostatic, induction, dispersion, and exchange-repulsion contributions, where the electrostatic and dispersion energies have their usual definitions in terms of intermolecular perturbation theory, but a new definition of the induction energy is used here. Instead of using the perturbative induction energy, which depends strongly on the basis set and is canceled to a large extent by the exchange-induction energy at short range, the SIMPER induction energy is now defined using a damped multipole series

$$E = -\sum_{n=6}^{16} C_n f_n(bR) R^{-n}. \quad (1)$$

The multipole coefficients C_n are obtained for the induction energy from molecular multipoles and polarizabilities, calculated up to maximum multipole rank $l=4$ with the same basis set as the corresponding MP2 supermolecule calculation. The functions f_n are *dispersion* damping functions and take the form of incomplete gamma functions. They are calculated[16] from the multipolar dispersion energy coefficients and the nonmultipolar perturbative dispersion energy. The advantage of using these dispersion damping functions to define the SIMPER induction energy is that the resulting induction energy is much more stable than the usual perturbative induction energy with respect to basis set variations. The SIMPER "exchange-repulsion" energy, which is simply the difference between the supermolecule energy and the sum of the electrostatic, induction, and dispersion energies, is also found to be less dependent on basis set.

For example, at an intermolecular geometry close to the global minimum, with a separation of $R=7.5\ a_0$ between the water oxygen atom and the midpoint of the CO bond, the dispersion energy coefficients at MP2/aug-cc-pVTZ supermolecule level are $C_6=70.0$, $C_7=181$, and $C_8=3206$ in units of bohr and hartree (the hartree E_h is approximately 4.359 744 aJ). Higher C_n, $n \leq 18$, are included in all calculations, but are not reported here for brevity. The total dispersion energy at MP2/aug-cc-pVTZ supermolecule level is $-1675\ \mu E_h$. This dispersion energy is equated to a damped multipole series taking the form of Eq. (1). To satisfy this equation, b must be $1.97\ a_0^{-1}$. The induction energy coefficients for this geometry, calculated at the same level of theory, are $C_6=9.2$, $C_7=64$, and $C_8=817$ (higher C_n up to C_{18} are also included), and substituting these into a damped multipole series of the form (1), with the same value of b, gives a SIMPER induction energy of $-481\ \mu E_h$. The convergence of the damped induction and dispersion energy series is fairly slow; they reach about 50% of the total energy when summed to the C_9 term and about 90% when summed to the C_{13} term. A direct perturbative calculation of the MP2/aug-cc-pVTZ electrostatic energy gives $-3833\ \mu E_h$, and the MP2 supermolecule interaction energy is calculated to be $-2652\ \mu E_h$. The SIMPER exchange-repulsion energy is obtained by subtracting the other three components (electrostatic, dispersion, and induction) from the supermolecule energy and is therefore $3337\ \mu E_h$. The same procedure is followed at every point on the surface to obtain the damping parameter b, and hence the induction and exchange-repulsion energies, as functions of the geometry and of the basis set.

The SIMPER "extrapolation" method is then applied in an attempt to improve the treatment of electron correlation in each of the four contributions to the interaction energy. The MP2 electrostatic energy is replaced by the electrostatic interaction between CCSD charge densities for the monomers calculated with the same basis set; this is $-3407\ \mu E_h$ in the example above. The MP2 dispersion and induction energy coefficients are replaced by coefficients obtained from CCSD multipoles and time-dependent coupled-cluster polarizabilities including orbital rotation effects.[19] The first three resulting dispersion energy coefficients are $C_6=66.5$, $C_7=230$, and $C_8=3718$, and the induction energy coefficients are $C_6=9.7$, $C_7=54$, and $C_8=656$ at the geometry considered above. The damping parameter b is replaced by the expression $b\sqrt{C_{6,\mathrm{CCSD}}C_{8,\mathrm{MP2}}/C_{6,\mathrm{MP2}}C_{8,\mathrm{CCSD}}}$,[16] where C_6 and C_8 are dispersion energy coefficients. This gives $b=1.781\ a_0^{-1}$. Substituting these values in Eq. (1), and including all coefficients up to C_{18}, gives a dispersion energy of $-1799\ \mu E_h$ and an induction energy of $-348\ \mu E_h$. Finally, the exchange-repulsion energy is assumed to be proportional to the charge density overlap integral. This decreases by about 6% from MP2/aug-cc-pVTZ to CCSD/aug-cc-pVTZ, so the exchange-repulsion energy is changed to $3139\ \mu E_h$. The sum of the four new components is the SIMPER interaction energy, which in this example is $-2416\ \mu E_h$ at the aug-cc-pVTZ level. This is less negative than the MP2 interaction energy mainly because of the change in the electrostatic interaction energy. The SIMPER method is usually found to be an improvement on the MP2 supermolecule method based on experimental evidence and data from higher-level supermolecule calculations, and SIMPER is not significantly more expensive than MP2, since no additional supermolecule calculations are needed. In this case, the CCSD(T)/aug-cc-pVTZ energy is $-2464\ \mu E_h$. This confirms that the MP2 method probably overestimates the depth of the potential well.

The effect of basis set incompleteness is then approximately corrected by performing MP2 and SIMPER calculations with the aug-cc-pVTZ and aug-cc-pVQZ basis sets and extrapolating the results to the complete basis set (CBS) limit. The results are available as supplementary material.[20] The error in the interaction energy calculated with a basis set of cardinality X (where $X=3$ and 4 for the two basis sets, respectively) is assumed to be proportional to $1/X^4$. The extrapolation is applied to the total interaction energy, not just to its correlation component, which is not easy to separate in the SIMPER method. However, the difference between the self-consistent field interaction energies calculated with the two basis sets is sufficiently small that extrapolating the total energy gives effectively the same result as extrapolating the correlation energy. Basis set extrapolation generally increases the binding energy. In the above example, the basis-set-extrapolated MP2 and SIMPER interaction energies are about $30\ \mu E_h$ more negative than the aug-cc-pVQZ interaction energies. This is a considerably smaller change than the effect of using SIMPER or CCSD(T) versus MP2 for the electron correlation, and therefore, since basis set incompleteness does not seem to be a major source of error in the calculations, alternative basis set extrapolation methods are not investigated.

The calculated potential energy surfaces are fitted to a sum of damped multipolar and short-range contributions. The damped multipolar energy consists of all terms in the multipole series (electrostatic, induction, and dispersion) expanded in multipole series centered on the oxygen atom of water and the geometric bond center of CO up to the R^{-8} term (the lowest term being the R^{-3} dipole-dipole interaction). This series (including the electrostatic energy) is damped, as shown in Eq. (1), using $b=2.0\ a_0^{-1}$ for computa-

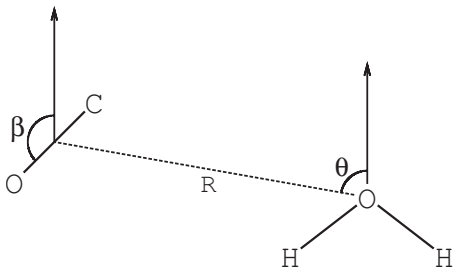

FIG. 1. Coordinate system used to describe planar H_2O-CO geometries. The arrows are parallel to the water symmetry axis.

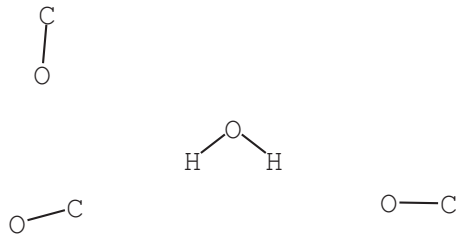

FIG. 2. The three equilibrium water-CO structures drawn with a single water molecule and three CO molecules representing the three symmetry-distinct equilibrium positions for CO relative to the water molecule. The O–H···C–O hydrogen-bonded dimer structure consists of the water molecule and the CO molecule at the lower left, the O–H···O–C hydrogen-bonded dimer structure consists of the water molecule and the CO molecule at the lower right, and the VDW dimer structure consists of the water molecule and the CO molecule at the upper left. The figure is drawn to scale for water and CO molecules in the equilibrium monomer geometries given in text.

tional convenience. This value of b is fairly close to the (orientation-dependent) dispersion damping parameters determined previously, and its precise value is found to make no significant difference to the fit. No fitting is therefore involved for this part of the energy. The short-range energy is obtained by subtracting the damped multipolar energy from the total interaction energy at each point. It is expressed as

$$E_{\mathrm{sr}} = e^{-bR}[f_{\mathrm{C}}(R_{\mathrm{O_W C}}, \Omega_{\mathrm{O_W C}}) + f_{\mathrm{O}}(R_{\mathrm{O_W O}}, \Omega_{\mathrm{O_W O}})], \qquad (2)$$

where $b=2.0\ a_0^{-1}$, O_W is the oxygen atom of water, and R is the distance between O_W and the center of the CO bond. The functions $f(R,\Omega)$ are linear combinations of 150 separate terms, each being a product of a power of distance (1, R, or R^2) with one of the 50 symmetry-allowed S-functions of orientation Ω,[21] up to $l=4$ on water and $l=2$ on the C and O atoms of CO. This gives a total of 300 coefficients that are fitted to the short-range energy for each of the 13 different water-CO pairs. The root mean square error in fitting these coefficients to over 10 000 calculated points is typically 20–25 μE_{h}, which is less than 1% of the well depth.

III. RESULTS

From SIMPER calculations extrapolated to the CBS limit, the minimum-energy geometry of the water-CO dimer is found to be planar, with the CO molecule located near a hydrogen atom of the water molecule, in an approximately linear O–H···C–O orientation. This result does not change qualitatively with other basis sets or when using the MP2 supermolecule method. Planar geometries can be defined by three coordinates (see Fig. 1): the distance R of a vector $\boldsymbol{R}$ from the water oxygen nucleus to the geometric center of the CO molecule, the direction θ of $\boldsymbol{R}$ measured anticlockwise from a vector z parallel to the symmetry axis of the water molecule (pointing from the H end to the O end), and the direction β of the bond vector of CO (pointing from C to O) measured anticlockwise from the direction of z. If the bond angle of water is x, then a perfect linear hydrogen bond is defined by $\theta=\beta=180°-x/2$.

However, when the CO bond is stretched, a different planar minimum is found with the oxygen atom of the CO molecule closest to the water molecule. The structure of this dimer is a distorted O–H···O–C hydrogen bond; a linear hydrogen bond would have $\theta=180°-x/2$ and $\beta=-x/2$. In addition, a planar "van der Waals" (VDW) minimum energy structure is found with the CO molecule close to the oxygen atom of water. Figure 2 shows examples of these three equilibrium structures and Table I lists the equilibrium geometries and interaction energies found for 12 combinations of water bond angle and CO bond length. The results in the table show the strong effect of CO bond length on the stability of the O–H···O–C and O–H···C–O dimer structures, which can be attributed to the change in direction of the CO dipole, from a positively charged oxygen end to a positively charged carbon end, when the molecule is stretched. This also supports the observation that the CO

TABLE I. Intermolecular geometry $(R/a_0, \theta/°, \beta/°)$ (defined in text) and intermolecular potential (in μE_{h}) of the water-CO dimer at planar equilibrium geometries denoted by HC (hydrogen bond to C atom of CO), HO (hydrogen bond to O atom of CO), and VDW (CO molecule near oxygen atom of water). The CO bond length is r and the water bond angle is x.

	$r=2.00\ a_0$	$r=2.175\ a_0$	$r=2.35\ a_0$
$x=80°$, HC	(7.30,146,140), −3731	(7.46,144,138), −2928	(7.64,141,134), −2087
$x=80°$, HO	(7.25,147,−40), −1475	(7.25,153,−35), −1987	(7.25,157,−33), −2485
$x=80°$, VDW	(6.02,16,104), −1351	(5.99,25,107), −1472	(6.25,45,−14), −1551
$x=100°$, HC	(7.26,122,113), −3357	(7.40,121,111), −2684	(7.54,116,105), −1977
$x=100°$, HO	(7.13,115,−81), −1386	(7.17,120,−78), −1779	(7.09,118,−91), −2168
$x=100°$, VDW	(6.05,59,171), −1385	(6.00,66,170), −1652	(5.84,66,158), −2088
$x=120°$, HC	(7.02,103,90), −3763	(7.14,99,86), −3069	(7.20,91,73), −2348
$x=120°$, HO/VDW	(6.75,90,−119), −1616	(6.80,94,−118), −1964	(5.83,65,163), −2423
$x=140°$, HC	(6.83,94,83), −4676	(6.96,92,81), −3847	(7.09,88,75), −2981
$x=140°$, HO/VDW	(6.74,89,−109), −1926	(6.75,89,−115), −2290	(6.35,79,−154), −2705

stretch vibration is blueshifted in CO–H_2O relative to the gas-phase CO value (Sec. I). When the bond angle of the water molecule increases toward linearity, the O–H···O–C and VDW structures become closer and eventually merge into a single minimum, denoted as "HO/VDW," and the stability of this structure usually decreases relative to the O–H···C–O structure.

At the equilibrium monomer geometries (not shown in the table), three minima are found with the most strongly bound being the O–H···C–O structure. This has a SIMPER/CBS binding energy of 2864 μE_h (where CBS refers to extrapolation to the complete basis set limit) compared to 1700 for the O–H···O–C hydrogen bond and 1638 for the "VDW" structure. The equilibrium structure and binding energy at the minimum agree well with previous studies (Sec. I). The local minima are about 20% more strongly bound in this work than in previous work,[6] which may be a result of basis set incompleteness in the earlier study, or of the different treatment of electron correlation.

As described above, water-CO interaction energies were calculated at 120 different geometries with the CCSD(T) method and the aug-cc-pVTZ basis set. Eighty-six of these energies are negative with the lowest being −2837 μE_h. The average absolute difference between these 86 CCSD(T) calculations and the MP2/aug-cc-pVTZ calculations is 206 μE_h, and the MP2 energies are on average more positive by 43 μE_h, even though the MP2 potential is more strongly bound at the minimum than the CCSD(T) potential. These differences between CCSD(T) and MP2 can be qualitatively explained. The dispersion energy is relatively underestimated by MP2, making the MP2 potential overall more shallow, but at the equilibrium structure the difference in the electrostatic energies outweighs the difference in dispersion.

The SIMPER/aug-cc-pVTZ potential is closer to the CCSD(T) potential with an average absolute difference of 78 μE_h between the two for the 86 negative-energy points. The SIMPER energies are on average more negative than the CCSD(T) energies by less than 1 μE_h; positive and negative differences between the two in different regions cancel almost exactly. The differences between SIMPER and CCSD(T) are thought to arise mainly from the treatment of short-range exchange repulsion by the SIMPER method, and accordingly, a greater difference between SIMPER and CCSD(T) is seen on the repulsive wall. The largest difference is 4400 μE_h, which is seen high on the repulsive wall where the interaction energy is about 40 000 μE_h. The MP2 and CCSD(T) energies differ by up to 1500 μE_h on the repulsive wall. However, these repulsive energies do not contribute significantly to the thermodynamic properties of the dimer at reasonable temperatures, since their Boltzmann factors are very small (40 000 $\mu E_h/k_B$ is over 12 000 K) and the volume of configuration space occupied by these regions of the repulsive wall is much smaller than the volume occupied by the potential well.

The barrier to proton exchange in the water-CO dimer, via a C_{2v} first-order saddle point with $\theta=180°$, is found to be 323 cm^{-1} for the equilibrium monomer geometries. Previous theoretical work[6] predicted that this barrier would be 283–293 cm^{-1}, and both this previous value and our result are significantly higher than the estimates of 210–230 cm^{-1} obtained from the analysis of spectroscopic data with a model Hamiltonian.[2,3] The dependence of the SIMPER/CBS barrier on intramolecular geometry is interesting. When the CO molecule is stretched, the barrier decreases, and when the CO bond length is 2.35 bohr and the water bond angle is 100°, the barrier is only 206 cm^{-1} for the O–H···C–O structure (through a $\theta=180°$, $\beta=180°$ barrier) and 121 cm^{-1} for the O–H···O–C structure (through a $\theta=180°$, $\beta=0°$ barrier), which is the equilibrium structure of water-CO when the CO is stretched. Clearly, a full description of the tunneling properties of this system will be complicated, as remarked by Oudejans and Miller.[5]

IV. SECOND VIRIAL COEFFICIENTS

A. Calculation

The cross second virial coefficient for the water-CO mixture is calculated with the procedure described previously,[17] including translational and rotational quantum effects to first order. The first-order quantum correction is only 8 $cm^3\ mol^{-1}$ at 200 K and less than 2 $cm^3\ mol^{-1}$ at 300 K, and higher-order quantum corrections should be negligible with respect to other uncertainties.

A first estimate of the effect of monomer vibration on the virial coefficients is also made. A set of rigid-monomer second virial coefficients $B_{12}(r,x;T)$ is first calculated for each of the 12 (r,x) pairs (excluding the pair with the monomers in their equilibrium geometries) from the fitted SIMPER/CBS potential energy surfaces, where r is the CO bond length and x is the water bond angle. These are then converted into second virial coefficients $B_{12}(v_1,v_2;T)$ for fixed monomer vibrational states, $v_1=0,1,2$ for the CO stretch and $v_2=0,1,2,3$ for the water bend. The averaging is done by diagonalizing suitable effective one-dimensional Hamiltonians for the vibrational modes, from the monomer MP2/aug-cc-pVQZ potential energy functions as described in Sec. II, and constructing a three-point integration scheme for CO and a four-point integration scheme for water based on the lowest-energy vibrational wave functions for each molecule. Finally, the cross second virial coefficient $B_{12}(T)$ is calculated from a Boltzmann average over the vibrational states.

The cross second virial coefficient is also calculated from the SIMPER/CBS potential energy surface for rigid monomers at their equilibrium geometries. This is found to agree well with the vibrationally averaged cross second virial coefficient; the difference is only about 1 $cm\ mol^{-1}$ at 300 K and 0.1 $cm\ mol^{-1}$ at 1000 K. Uncertainties in the potential energy surfaces give much larger uncertainties in the second virial coefficients (see below). Hence, a more accurate calculation of the effect of vibrational averaging is probably not worth the additional effort at present.

The vibrationally averaged B_{12} values are fitted as a function of temperature,

TABLE II. Coefficients for Eq. (3) for $B_{12}(T)$ for the H_2O/CO pair. The c_i are in $cm^3\ mol^{-1}$ and the d_i are dimensionless.

i	c_i	d_i
1	493.709	−0.45
2	−579.466	−0.57
3	−248.146	−2.00
4	−271.885	−4.25

$$B_{12}(T) = \sum_{i=1}^{4} c_i (T^*)^{d_i}, \tag{3}$$

where $T^* = T/(100\ \mathrm{K})$, B_{12} and the c_i have units of $cm^3\ mol^{-1}$, and the values of c_i and d_i are given in Table II. Equation (3) reproduces the calculated values within a tolerance that is much smaller than their uncertainty. It is valid from 200 to 2000 K and extrapolates in a physically reasonable manner beyond that range. Table III shows the calculated values of $B_{12}(T)$, along with their expanded uncertainties computed as described in the following paragraph.

An estimate of the uncertainty in the virial coefficients is obtained by multiplying the negative SIMPER/CBS interaction energies by 1.07 and dividing the positive interaction energies by 1.07, to give a lower bound on the virial coefficients, and vice versa, to give an upper bound. (The small R^{-3} dipole-dipole interaction is excluded from this scaling because scaling it in this way would introduce an isotropic R^{-3} contribution into the energy, which would cause the classical second virial coefficient to diverge.) The value of 1.07 is based on the average absolute difference of 78 μE_h seen between CCSD(T) and SIMPER calculations for a number of points in the potential well (Sec. III), for which the average CCSD(T) interaction energy is about −1100 μE_h. The virial coefficients calculated from the SIMPER and CCSD(T) methods are expected to agree more closely than this, however, because the SIMPER energies are above the CCSD(T) energies in some regions and below them in others, giving a cancellation of errors in the virial coefficients. Of course, neither SIMPER nor CCSD(T) reproduces the correlation energy exactly. We conservatively consider these uncertainty bounds to represent an expanded uncertainty with coverage factor $k=2$, approximately equivalent to a 95% confidence interval.

TABLE III. Second virial coefficients B_{12} calculated with Eq. (3) and their expanded uncertainties $U(B_{12})$.

T (K)	B_{12} ($cm^3\ mol^{-1}$)	$U(B_{12})$ ($cm^3\ mol^{-1}$)
200	−105.2	22.7
250	−62.1	14.9
300	−38.8	11.0
350	−24.4	8.8
400	−14.6	7.3
450	−7.7	6.3
500	−2.5	5.5
600	4.7	4.5
700	9.4	3.8
800	12.6	3.3
900	15.0	2.9
1000	16.7	2.7
1500	21.1	1.9
2000	22.6	1.5

TABLE IV. H_2O/CO second virial coefficients derived from experimental data (Ref. 22).

T (K)	B_{12} ($cm^3\ mol^{-1}$)	Uncertainty in B_{12} ($cm^3\ mol^{-1}$)
310.92	−61.6	5.2
366.46	−30.2	6.3
422.00	−19.3	8.3
477.55	3.0	15.5

B. Comparison to experimental data

Experimental data for B_{12} for H_2O/CO are scarce. Gillespie and Wilson[22] measured the solubility of liquid water in carbon monoxide gas (and the coexisting liquid composition) at four temperatures. Values for B_{12} and their uncertainties were derived from these data by methods described previously.[23] The results are given in Table IV. The uncertainties in the table (expanded uncertainties with coverage factor 2) reflect only the measurement of water content in the gas phase; additional factors such as neglect of higher virial coefficients are not included.

Vapor-phase enthalpy-of-mixing data, when extrapolated to low pressure, yield the quantity $\phi_{12} = B_{12} - T(dB_{12}/dT)$. At temperatures from approximately 363 to 403 K, values of ϕ_{12} were reported by Smith and Wormald[24] and reanalyzed by Wormald and Lancaster.[25] In Table V we give the results from the reanalysis along with their reported uncertainties.

At higher temperatures and pressures, excess enthalpies for this mixture were reported by Lancaster and Wormald,[26] who reanalyzed earlier measurements.[28] Similar data were reported at two temperatures by Wilson and Brady.[27] As described previously,[23] we extrapolated these data to zero pres-

TABLE V. Values of $\phi_{12} = B_{12} - T(dB_{12}/dT)$ for H_2O/CO derived from vapor-phase enthalpy-of-mixing data.

T (K)	ϕ_{12} ($cm^3\ mol^{-1}$)	Uncertainty in ϕ_{12} ($cm^3\ mol^{-1}$)	Reference
363.48	−100	16	25
375.17	−96	24	25
393.17	−79	16	25
403.17	−89	22	25
473.16	−32	26	26
523.16	−54	31	26
573.16	−22	25	26
585.0	−56	37	27
623.16	−31	17	26
648.16	−15	13	26
673.16	−17	13	26
690.5	−47	17	27

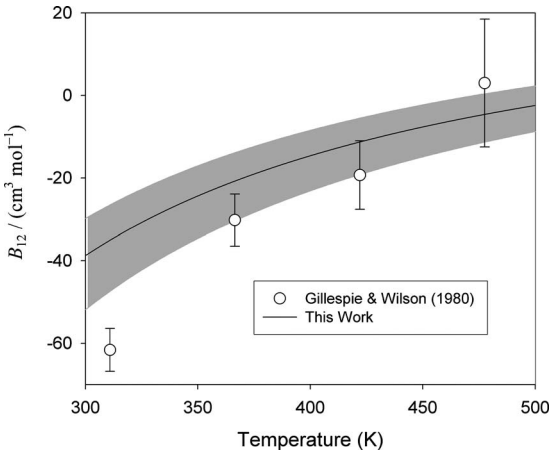

FIG. 3. Comparison of values of B_{12} calculated in this work with values derived from experimental data. The shading represents the expanded ($k=2$) uncertainty in the calculated results.

sure in order to extract ϕ_{12}. These values are also given in Table V; their uncertainties arise primarily from uncertainty in the zero-pressure extrapolation.

For all calculations, $B(T)$ and dB/dT for pure water were calculated from the correlation of Harvey and Lemmon.[29] Properties of pure carbon monoxide, including $B(T)$, were calculated from the equation of state of Lemmon and Span.[30]

In Fig. 3, we show our calculated values of B_{12} along with the limited experimental data. The shaded area represents the uncertainty in our results; this uncertainty is based on calculations with the SIMPER potential perturbed to be more positive and more negative by 7% as explained above. Both our uncertainties and those of the literature points may be taken as expanded uncertainties with coverage factor $k=2$ (approximately a 95% confidence interval). Agreement with the data of Gillespie and Wilson[22] is reasonable except for their lowest-temperature point. We note that the similar low-temperature point from Ref. 22 was also an outlier in the same direction in our earlier work on the water-hydrogen system.[17]

Figure 4 shows a similar comparison with the quantity

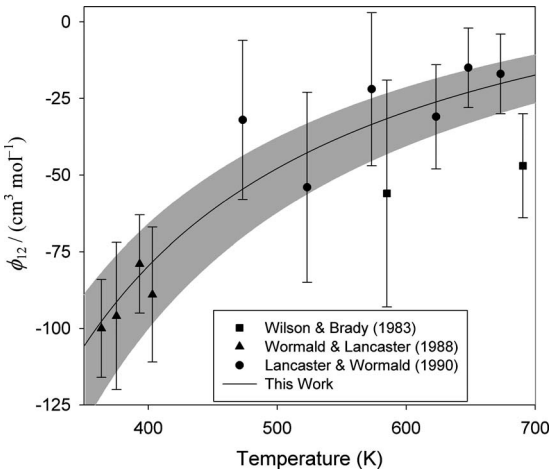

FIG. 4. Comparison of values of ϕ_{12} calculated in this work to values derived from experimental data. The shading represents the expanded ($k=2$) uncertainty in the calculated results.

ϕ_{12} defined above. For this property, the agreement with available experimental data[26–28] is excellent. We note that because ϕ_{12} contains the derivative dB_{12}/dT, it would be difficult for the $B_{12}(T)$ function to pass through all the experimental points in Fig. 3 without spoiling the good agreement in Fig. 4.

V. CONCLUSIONS

The properties of weakly bound molecular complexes are usually sensitive to the interaction energy over a range of different geometries, not just around the minimum. Although the equilibrium structure and energy of the water-CO dimer have been known for some time, this work has revealed a number of new features. These include the strong dependence of the interaction energy on the CO bond length, which is a result of the changing dipole of the CO molecule. The qualitative features of the seven-dimensional potential energy surface are the same for MP2, CCSD(T), and SIMPER calculations, and for several different basis sets, so they are expected to be realistic.

As might be expected, the structure and energy of the water-CO dimer are similar to the isoelectronic water-N_2 dimer, since both are planar and hydrogen bonded, although water-CO is rather more strongly bound with a SIMPER/CBS binding energy of 2864 μE_h compared with 2009 μE_h for water-N_2.[18] Both dimers also feature more weakly bound planar VDW minima, where the diatomic molecule is close to the oxygen atom of water, although at the water-N_2 VDW local minimum the nitrogen molecule is placed symmetrically on the water axis, whereas the CO molecule is well off the axis. The lower symmetry of the CO molecule also gives rise to a third water-OC local minimum in which the O atom of CO is "hydrogen bonded" to an H atom of water.

Second virial coefficients for the water-CO mixture have been calculated and are slightly more negative than calculated water-N_2 second virial coefficients,[18] although the difference is not large, especially at high temperatures, despite the stronger binding of CO to water at the minimum. This suggests that there are regions of the potential energy surface where the CO molecule is less strongly bound to water than a nitrogen molecule would be (for example, the water-OC hydrogen bonded dimer is bound by only about 1700 μE_h). The calculated second virial coefficients cover a much wider range of temperatures than the limited experimental data, and their estimated uncertainties are smaller at higher temperatures. Although the water-CO potential energy surface depends significantly on the monomer geometries, the estimated effect of averaging over monomer vibrations gives second virial coefficients similar to those obtained from only the equilibrium monomer geometries.

ACKNOWLEDGMENTS

The authors thank E. W. Lemmon for assistance in fitting Eq. (3). Partial financial support for this work was provided by the Electric Power Research Institute and by the Engineering and Physical Sciences Research Council. This

work is a partial contribution of the National Institute of Standards and Technology, not subject to copyright in the United States.

[1] Electric Power Research Institute, EPRI Report No. 1015542, 2008.
[2] D. Yaron, K. I. Peterson, D. Zolandz, W. Klemperer, F. J. Lovas, and R. D. Suenram, J. Chem. Phys. **92**, 7095 (1990).
[3] R. E. Bumgarner, S. Suzuki, P. A. Stockman, P. G. Green, and G. A. Blake, Chem. Phys. Lett. **176**, 123 (1991).
[4] M. D. Brookes and A. R. W. McKellar, J. Chem. Phys. **109**, 5823 (1998).
[5] L. Oudejans and R. E. Miller, Chem. Phys. Lett. **306**, 214 (1999).
[6] J. Sadlej and V. Buch, J. Chem. Phys. **100**, 4272 (1994).
[7] J. Sadlej, B. Rowland, J. P. Devlin, and V. Buch, J. Chem. Phys. **102**, 4804 (1995).
[8] A. F. A. Vilela, P. R. P. Barreto, R. Gargano, and C. R. M. Cunha, Chem. Phys. Lett. **427**, 29 (2006).
[9] J. Lundell and Z. Latajka, J. Mol. Struct. **887**, 172 (2008).
[10] T. H. Dunning, J. Chem. Phys. **90**, 1007 (1989).
[11] E. M. Mas and K. Szalewicz, J. Chem. Phys. **104**, 7606 (1996).
[12] G. Herzberg, *Molecular Spectra and Molecular Structure I. Spectra of Diatomic Molecules* (Van Nostrand, Princeton, 1950).
[13] R. J. Wheatley and A. H. Harvey, J. Chem. Phys. **127**, 074303 (2007).
[14] MOLPRO, a package of *ab initio* programs designed by H.-J. Werner and P. J. Knowles, version 2002.6, R. Lindh, F. R. Manby, M. Schütz *et al.*
[15] Certain commercial products are identified in this paper, but only in order to adequately specify the procedure. Such identification neither constitutes nor implies recommendation or endorsement by either the U.S. government or the National Institute of Standards and Technology.
[16] E. Bichoutskaia, A. S. Tulegenov, and R. J. Wheatley, Mol. Phys. **102**, 567 (2004).
[17] M. P. Hodges, R. J. Wheatley, G. K. Schenter, and A. H. Harvey, J. Chem. Phys. **120**, 710 (2004).
[18] A. S. Tulegenov, R. J. Wheatley, M. P. Hodges, and A. H. Harvey, J. Chem. Phys. **126**, 094305 (2007).
[19] R. J. Wheatley, J. Comput. Chem. **29**, 445 (2008).
[20] See EPAPS supplementary material at http://dx.doi.org/10.1063/1.3244594 for MP2 and SIMPER interaction energies extrapolated to the complete basis set limit.
[21] A. J. Stone and R. J. A. Tough, Chem. Phys. Lett. **110**, 123 (1984).
[22] P. C. Gillespie and G. M. Wilson, Gas Processors Association Report No. RR-41, 1980.
[23] M. P. Hodges, R. J. Wheatley, and A. H. Harvey, J. Chem. Phys. **117**, 7169 (2002).
[24] G. R. Smith and C. J. Wormald, J. Chem. Thermodyn. **16**, 543 (1984).
[25] C. J. Wormald and N. M. Lancaster, J. Chem. Soc., Faraday Trans. 1 **84**, 3141 (1988).
[26] N. M. Lancaster and C. J. Wormald, J. Chem. Eng. Data **35**, 11 (1990).
[27] G. M. Wilson and C. J. Brady, Gas Processors Association Report No. RR-73, 1983.
[28] C. J. Wormald, N. M. Lancaster, and A. J. Sellars, J. Chem. Thermodyn. **18**, 135 (1986).
[29] A. H. Harvey and E. W. Lemmon, J. Phys. Chem. Ref. Data **33**, 369 (2004).
[30] E. W. Lemmon and R. Span, J. Chem. Eng. Data **51**, 785 (2006).